J MATER SCI **41** (2006) 2449–2455

Stress relaxation in bending of AISI 316 at 773 K

F. POVOLO
Unidad de Actividad Materiales CAC–CNEA, Av. Gral Paz 1499, 1650 San Martín, Argentina; CONICET, Av. Rivadavia 1917, 1033, Buenos Aires, Argentina

G.A. MANSILLA*
UTN – Facultad Regional San Nicolás, Colón 332, 2900 San Nicolás, Argentina
E-mail: gmansilla@frsn.utn.edu.ar

É. B. HERMIDA
Unidad de Actividad Materiales CAC–CNEA, Av. Gral Paz 1499, 1650 San Martín, Argentina; CONICET, Av. Rivadavia 1917, 1033, Buenos Aires, Argentina

Published online: 3 March 2006

In this article, stress relaxation in bending of AISI 316 stainless steel at 773 K during 490 hours is characterized. Samples were cut either parallel or transverse to the rolling direction and treated at different temperatures prior to the bending tests. The mechanical behavior shown by the longitudinal samples is quite different from that of the transverse samples and so we conclude there must be differences at the level of their microstructures. However, the presence of sigma phase precipitates in both cases is the consequence of a stress-assisted process. Besides, intragranular carbide density in either sample proved to be a function of the relaxation time.

1. Introduction

Recently, Nabarro [1] added a worthy contribution to the discussion around the mechanisms concerned with creep at very low strain rates (less than 10^{-11} s^{-1}). He proposed that deformation occurs by the migration of vacancies rather than by a dislocation glide. Earlier Lifshitz [2] suggested, in a continuous model for diffusional creep, that grain boundary sliding should necessarily occur. He also pointed out that two simultaneous sliding processes should be considered, i.e. a grain boundary sliding promoted by diffusional processes and another that would accommodate these diffusional processes. On the other hand, Langdon [3] demonstrates that in the region of low stresses the Harper-Dorn creep and grain boundary sliding are operative creep mechanisms.

It is well known that during creep tests dislocations do move inside the grains and that also grain boundaries migrate. Precipitation in practical engineering materials represents an important mechanism for anchoring grain boundaries and thus decreasing plastic deformation. However, individual polycrystalline grains may become displaced during high temperature creep. Mechanisms such as dynamic strain ageing cause an increased rate of dislocation multiplication, which delays the recovery of the dislocation structure. At 773 K, stainless steel type AISI 316 shows dynamic strain ageing due to the presence of substitutional solutes. Nowadays a complete description and interpretation of dynamic strain ageing phenomena can be found in [4].

We believe that although AISI 316 has been widely investigated already, in these last years there have been very few papers concerning its stress relaxation behavior. Some papers do establish relationships between its mechanical properties and its microstructure, but neither temperature nor stress dependence have been considered up to now. Most papers are devoted to tertiary creep [5] and to the discussion of proper methods for calculating the Monkman-Grant parameters.

Thus, the aim of this paper is to achieve a better understanding of the stress relaxation behavior of AISI 316 L at 773 K, at very low strain rates, and its dependence on texture and on the thermal treatments received.

2. Theoretical background

Two of the most useful theoretical expressions considered when relating the stress-relaxation or creep data to elementary dislocation models, are the Johnston-Gilman and Hart equations. On the one hand Johnston and Gilman described the plastic strain rate $\dot{\varepsilon}$ produced by dislocations that move with a mean velocity $\bar{v}$, when the applied stress

*Author to whom all correspondence should be addressed.
0022-2461
DOI: 10.1007/s10853-006-5152-8

σ is greater than the minimum stress required to move dislocations, σ_i. The model is summarized by the following constitutive equation [7]:

$$\dot{\varepsilon} = \phi\rho b\bar{v} = \frac{\phi\rho b v_o}{\sigma_0^m}(\sigma - \sigma_i)^m \equiv \frac{\dot{\varepsilon}_{JG}}{\sigma_0^m}(\sigma - \sigma_i)^m = \dot{\varepsilon}_0(\sigma - \sigma_i)^m \quad (1)$$

where ϕ is the orientation factor of the slip system, ρ is the density of mobile dislocations that move with the mean velocity $\bar{v}$, b is the Burgers vector and $\bar{v}_0$, σ_0 and m are material constants.

On the other hand, Hart interpreted the relaxation curves in terms of a state variable approach. At high homologous temperatures the $\log\sigma - \log\dot{\varepsilon}$ curves can be represented by [8]:

$$\dot{\varepsilon} = \dot{\varepsilon}_H \ln\left(\frac{\sigma}{\sigma^*}\right)^{-1/\lambda} \quad (2)$$

where σ^* is a hardness parameter, λ is a temperature independent parameter and $\dot{\varepsilon}_H$ depends on temperature, heat treatment and deformation. Furthermore, the internal stress can be calculated as [9]

$$\sigma_i = \sigma - \sigma_0\left[\ln\left(\sigma^*/\sigma\right)\right]^{-1/\lambda m} \quad (3)$$

If relationships (1) and (2) are plotted in a $\log\sigma - \log\dot{\varepsilon}$ diagram, two distinct curvatures are found: one of them concave upwards, equation (1) and the other one concave downwards, equation (2). When the $\log\sigma - \log\dot{\varepsilon}$ curve of experimental data presents a double curvature, both models are applied [9]. The characteristic parameters of the Johnston-Gilman equation, m, $\dot{\varepsilon}_{J-G} = \phi\rho b v_o$,$\sigma_0$ and σ_i, or those of the Hart model, λ, $\dot{\varepsilon}_H$ and σ^*, determined by a proper fit of relaxation data will be correlated with the respective microstructure of AISI 316 L samples.

3. Experimental procedure

3.1. Sample preparation

The original material was supplied by a Finish company in the form of a 0.6 mm thick sheet and in a mildly annealed condition. Table I gives the typical composition of the AISI 316 L alloy.

Two sets of specimens were cut. The first one was cut with its axis parallel to (that is, longitudinal to) the rolling direction and the second was cut with its axis perpendicular to (that is, transverse to) the rolling direction. Each sample was 100 mm long and 10 mm wide. Samples were carefully cleaned with detergent, rinsed with water, immersed in isopropyl alcohol and blow-dried. Both the longitudinal and the transverse samples were separated in four groups of ten samples. Each group of samples was sealed into fused silica tubes with an argon atmosphere in order to avoid oxidation during heating. Table II presents the temperatures of the heat treatments chosen to dissolve the different precipitates.

It is worth mentioning that after each thermal treatment all specimens (including those named *as received*) were heated and cooled in air for 1 hour at 823 K, in order to release internal stresses.

TABLE I: Composition of AISI 316 L alloy

C	Cr	Ni	Mo	Mn	P	S	N	Si	Fe
.032	17.2	10.7	2.57	1.50	.032	.01	.044	.65	balance

TABLE II. Thermal treatments prior to the bending tests

Type AR	Temperature (K) As received	Time (hours)	Cooling media
A	1172	1	water
B	1203	1	water
C	1253	1	water

3.2. Stress relaxation in bending

Bending is a very useful technique to determine quasistatic mechanical properties, in particular the elementary dislocation involved in plastic deformation. In fact, the influence of a broad set of variables such as composition, thermo mechanical treatments, etc, can be evaluated simultaneously through this technique. Furthermore experimental data are obtained up to times of the order of those reached in creep. The procedure consists of locating flat specimens in a holder with a specific curvature [10]. This curvature will determine the initial stress applied to the outer surface; hence the holder is usually labeled by the holder stress Σ.

In our tests we consider three different holders characterized by the following initial stresses: 210 MPa, 171 MPa and 137 MPa. In each holder we dispose two samples corresponding to each heat treatment (AR, A, B and C). In all, we put eight specimens per holder, inserted into a furnace at the selected temperature (773 $\pm$ 1) K and controlled with thermocouples attached to the holders. Periodically we extract the samples out of the holders to measure the remnant curvature using a profile projector; duplicate specimens helped us evaluate the dispersion between the curvatures corresponding to samples with the same thermal treatment.

The stress at the surface of a sample bent inside the holder is [11]:

$$\sigma_b = \frac{Eh}{2}\left(\frac{1}{R} - \frac{1}{R_i}\right) \quad (4)$$

where $E = 166$ GPa is the elastic modulus of the AISI 316 at 773 K [12], R the radius of the holder, h the thickness of the specimen and R_i the curvature of the

sample when released from the holders after a relaxation time t_i.

The stress at the surface of the bent specimen before unloading, σ_b, can be correlated with the homogeneous stress of a sample submitted to an uniaxial test, σ, by the relationship [11]:

$$\sigma = \frac{2}{3}\sigma_b + \frac{\Sigma}{3}\frac{d\sigma_b}{d\Sigma} \tag{5}$$

where $\Sigma = Eh/2R$ is the stress imposed by the holder at the surface of the bent specimen. For evaluating $d\sigma_b/d\Sigma$ holders with different radii were employed.

3.3. Metallographic characterization

Microstructural analyses were preformed before bending tests with the aim of controlling precipitates development during heat treatments. After the relaxation tests the microstructure of the samples was observed again using metallographic and scanning electron microscopes. Samples were polished carefully and then etched in order to reveal the general structure and the precipitates. Because its crystalline structure is tetragonal, the sigma phase responded to crossed polarized light blinking and, when observed under this kind of light, looks like light-blue lagoons. Also we found titanium carbides which shine with crossed polarized light, but do not sparkle.

The semi-quantitative chemical composition of the precipitates was determined by means of Energy Disperse Spectra (EDS) analyzer attached to the scanning electron microscope.

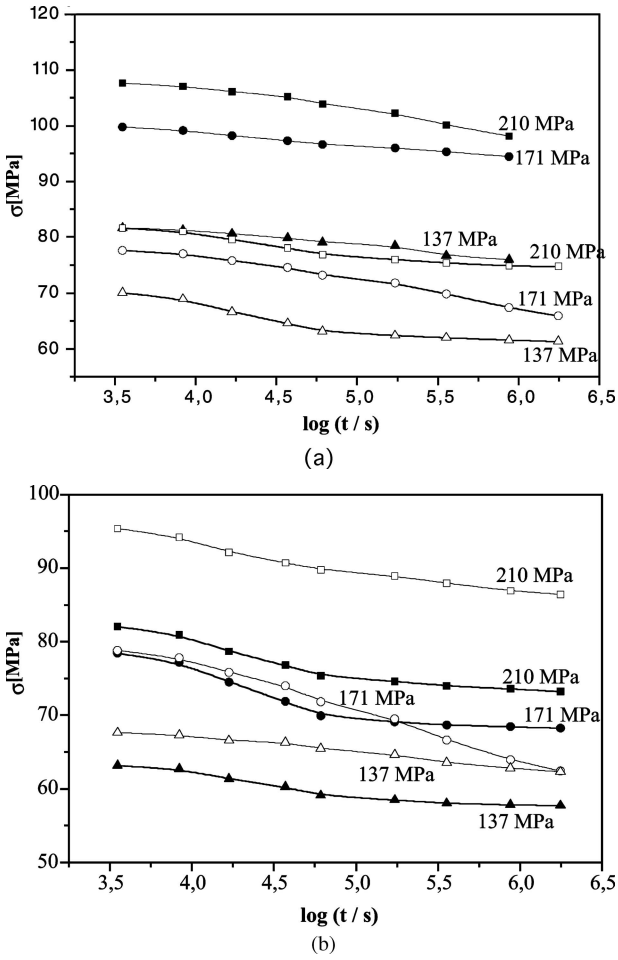

Figure 1. (a) - Stress – time curves for the longitudinal samples *as received* (full symbols) and with the heat treatment A (open symbols) (b) Stress - time curves corresponding to the longitudinal samples subjected to the heat treatment B (full symbols) and those corresponding to treatment C (open symbols). The labels in curves indicate the holder stress

4. Results

4.1. Relaxation tests

Figures 1 and 2 show the stress relaxation curves for the different heat treatments for longitudinal and transverse samples. In order to fit these data with the phenomenological equations (1) or (2) these data should be plotted in a $\log\sigma - \log\dot{\varepsilon}$ diagram. This can be easily done on considering that the plastic strain rate is $\dot{\varepsilon} = -\frac{\dot{\sigma}}{E}$, where E is the elastic modulus and the dot indicates the derivative with respect to the relaxation time [9].

4.1.1. Longitudinal samples

Figures 3 (a) and (b) illustrate the relaxation behavior of the longitudinal samples exposed to different heat treatments before the bending tests. Relaxation curves show clearly two different types of curvatures. Those concave upwards were fitted by the Johnston-Gilman equation [9, 12], while the branch of the Hart equation for high homologous temperatures was used to fit the concave downwards curves. For the case of the double curvature, observed in the relaxation of longitudinal samples with thermal treatment *C* disposed in the holders with the lowest stresses, both equations were used to get a proper fit (see Table III).

Stress relaxation of the samples as received, exposed to stresses of 137 MPa and 171 MPa were quite linear when plotted in a $\log\sigma - \log\dot{\varepsilon}$ diagram. Thus, these curves can be fitted by equation (1) on assuming that $\sigma \gg \sigma_i$, which would mean we are at the beginning of the relaxation process [13]. Then, if we neglect the contribution of the internal stress, for those curves we can determine the parameter m and the factor $\dot{\varepsilon}_{J-G}/\sigma_0^m$.

4.1.2. Transverse samples

A quite different mechanical response was obtained from transverse samples, as shown in Figs. 2(a) and (b). The relaxation begins at higher stresses than those observed for the longitudinal samples, certainly due to the differences in texture.

Figure 4(a) shows clearly the anomalous relaxation behavior of the material (as received) bent under an initial stress of 137 MPa. The relaxation curve is linear, so

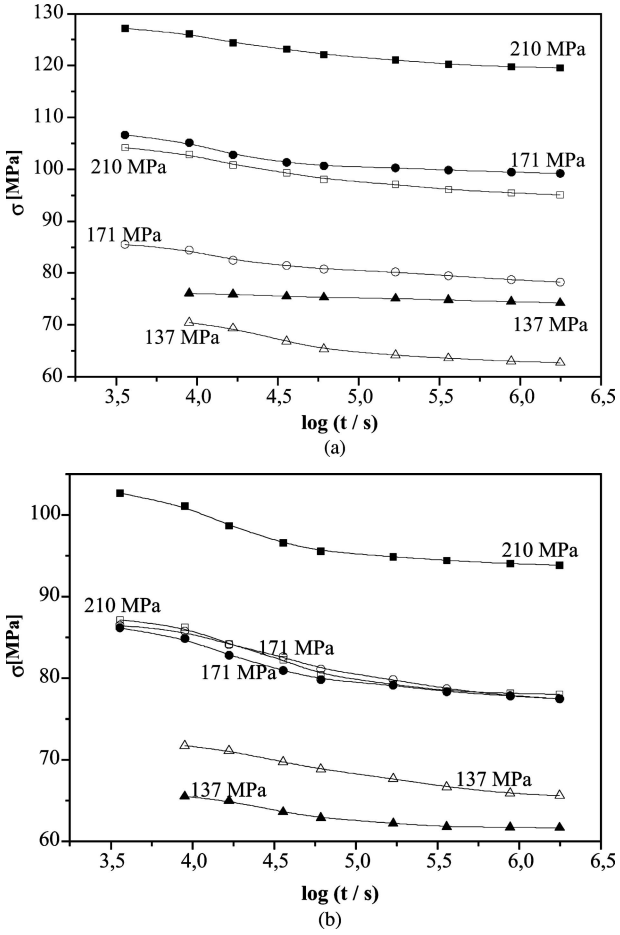

Figure 2. (a) Stress – time curves for the transverse samples *as received* (full symbols) and with the heat treatment A (open symbols); (b) Stress - time curves corresponding to the transverse samples exposed to the heat treatment B (full symbols) and those corresponding to treatment C (open symbols). The labels in curves indicate the holder stress

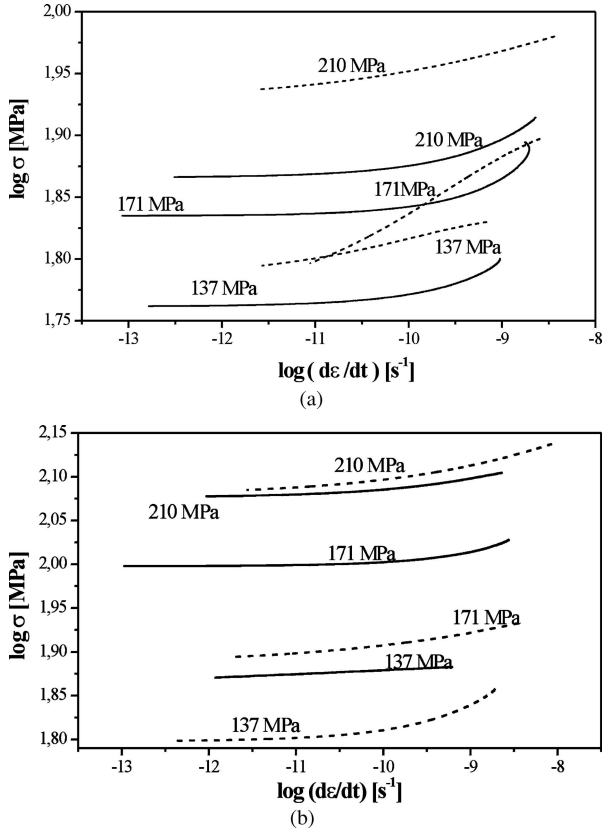

Figure 3. (a) - Relaxation curves for longitudinal samples as received (full line) and with the heat treatment A (dashed line); (b) Relaxation curves corresponding to the longitudinal samples subjected to the heat treatments B (full line) and C (dashed line). The labels in curves indicate the holder stress

equation (1) does fit the experimental data if we neglect the internal stress. From these data it is impossible for us to specify whether the movements of the dislocations held during the relaxation directly involve interactions with the precipitates present in these samples.

All other curves are concave upwards, and so the Johnston-Gilman equation is employed to fit the data, yielding the parameters shown in Table IV.

Relaxation of the transversal samples can be divided into two groups, according to the stress exponent: one group includes samples with m = 3 and the other includes samples with m = 2, independently of the thermal treatment received by the samples. The relaxation of

TABLE III. Fitting parameters for the relaxation of the longitudinal samples

		Johnston-Gilman			Hart		
Type	Σ [MPa]	m	$\dot{\varepsilon}_{J-G}/\sigma_0^m$ [x 10^{-11} s^{-1}.MPa^{-m}]	σ_i [MPa]	λ	$\dot{\varepsilon}^*$ [s^{-1}]	$\sigma*$ [MPa]
AR	210				0.2	1.5 10^{-16}	111
	171	115	10^{-233}	—			
	137	92	10^{-177}	—			
A	210	1.8	4	75			
	171				0.13	2 10^{-15}	93
	137	1.9	4	61			
B	210	2.0	3	73			
	171	1.9	5	68			
	137	1.6	8	58			
C	210	4.9	2. 10^{-3}	84			
	171	4.4	5. 10^{-5}	54	0.2	6 10^{-15}	91
	137	3.4	0.2	58	0.18	4 10^{-16}	73

TABLE IV. Johnston–Gilman parameters for transverse samples, thermal treatments are indicated

Type	Σ [MPa]	$\dot{\varepsilon}_{J-G}/\sigma_0^m$ [x 10^{-11} $s^{-1}.MPa^{-m}$]	m	σ_i [MPa]
AR	210	1	3	119
	171	4	2	99
A	210	0.2	3	120
	171	0.5	3	78
	137	2	2	63
B	210	4	2	94
	171	4	2	78
	137	5	2	51
C	210	4	2	78
	171	0.4	3	77
	137	0.7	3	64

the transverse samples (as received), tested at 137 MPa, was fairly linear and therefore no internal stress could be determined.

4.2. Metallographic observations

The comparison of the microstructure observed before and after each heat treatment allows us to say that the microstructure is free of precipitates before the bending tests. Furthermore, it is characterized by two grain sizes (22 and 32 μm) and some grains exhibit twins. After the stress relief treatment (performed to all samples including those named *as received*) before bending the microstructure shows a remarkable grain enlargement, and no precipitates. Keeping in mind that this last treatment was performed at 823 K during 1 hour and air cooled, from the transformation alloy curves no precipitates are expected. This agrees with the metallographic observations as shown in Fig. 5.

Besides, carbide density grows as the relaxation time increases which can be proved comparing microstructures before and after relaxation tests. This fact can be explained if we consider that dislocations created during relaxation act as carbides nucleation sites.

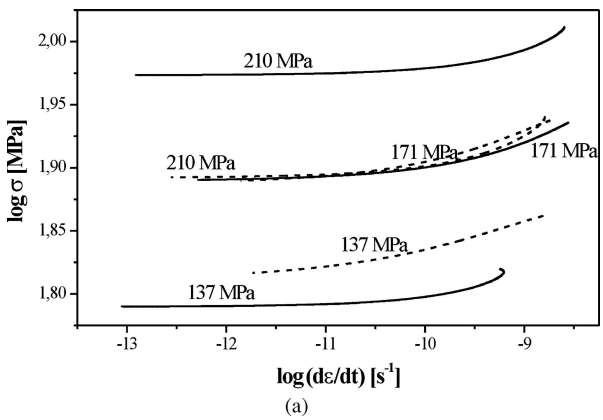

(a)

Figure 4. Relaxation curves for transversal samples: (a) material *as received* (full line) and treatment B (dashed line); (b) samples exposed to heat treatments B (full line) and C (dashed line). The labels indicate the holder stress

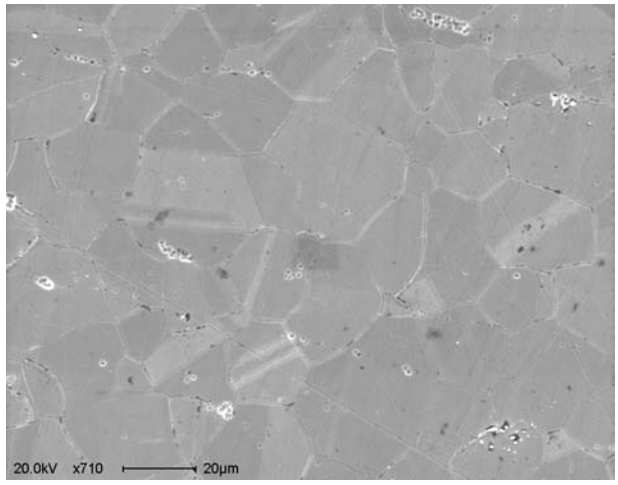

Figure 5. Secondary electron micrograph of longitudinal samples corresponding to *as received* samples, the microstructure is characterized by two grain sizes and twins inside the grains

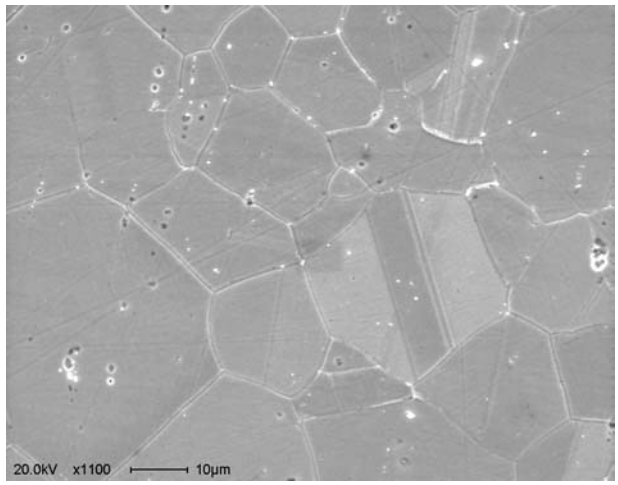

Figure 6. Secondary electron micrograph depicting small (particle's sizes less than 1 micron) dispersion of $M_{23}C_6$ carbides inside the grains and at grain boundaries for longitudinal sample subjected to thermal treatment C bent at 171 MPa

4.2.1. Longitudinal samples

According to the alloy time-temperature-composition diagram [14], in AISI 316 heated at 773 K during 490 h only $M_{23}C_6$ particles are expected to appear as precipitates. Nevertheless, recent studies [15] show the existence of four distinct precipitation stages in 316 L between 673 K and 773 K, which involve sigma phase precipitation and the formation of $M_{23}C_6$ carbides after a 24 hour aging. This agrees with the microstructure of our samples; titanium carbides at grain boundaries, and Cr and Mo carbides of the type $M_{23}C_6$ are mainly found inside the grains, as seen in Fig. 6. Besides these precipitates, in the samples as received bent at holder stress of 210 MPa and in those subjected to the heat treatment A tested into the holder of 171 MPa we found sigma phase particles (with a size greater than 3 μm) both inside the grains and at grain boundaries as shown in Fig. 7.

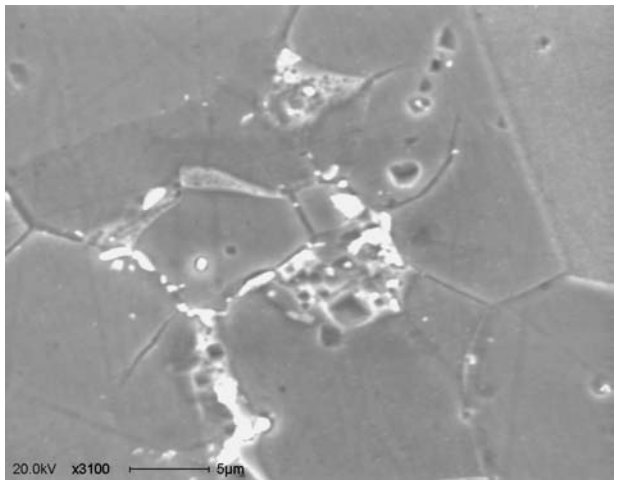

Figure 7. Scanning micrograph showing coarse sigma phase precipitates at grain boundaries as well as inside them associated to longitudinal samples relaxed at 171 MPa after heat treatment A

The presence of sigma phase can be explained as a temperature/stress assisted phenomena, where the temperature used during the stress relaxation is the main cause of the generation of this microstructure. Besides, the presence of silicon in the chemical composition also promotes the formation of sigma phase.

4.2.2. Transverse samples

From a microstructural analysis we can consider two perfectly different groups of samples: one characterized by very fine dispersions of Titanium carbides and $(Cr,Mo)_{23}C_6$ mainly located inside the grains, as illustrated in Fig. 8, and a second group which includes samples with very small sigma phase precipitates (1 micron) not expected, as explained above, nucleated preferently at grain boundaries even when some particles were found inside the grains, exhibited in Fig. 9.

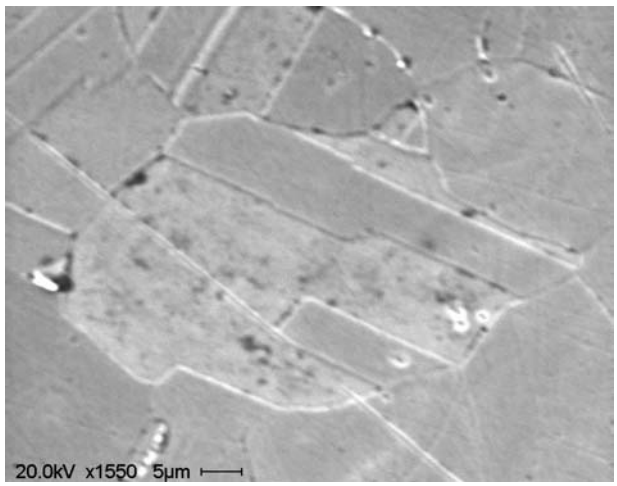

Figure 8. Secondary electron micrograph depicting $(Cr, Mo)_{23}C_6$ particles (dark) and sigma phase precipitates (white) at grain and twin boundaries as well as inside the grains – transverse sample relaxed 210 MPa after heat treatment A

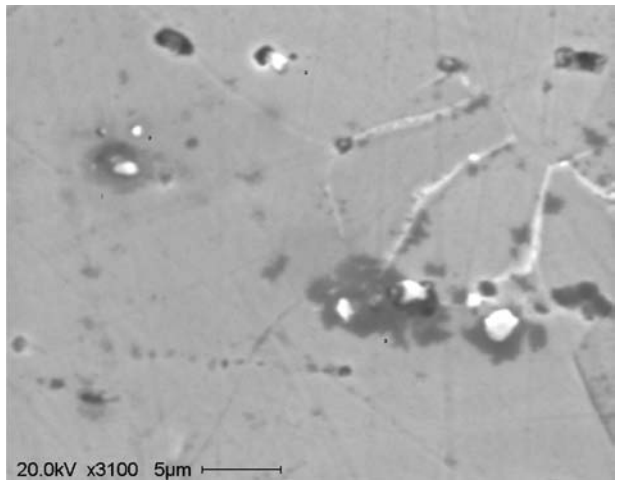

Figure 9. Secondary electron micrograph developed by transverse samples subjected to heat treatment B and bent at 210 MPa: 1 - $M_{23}C_6$ chromium rich carbides, 2 - sigma phase precipitates and 3 - titanium carbides

5. Discussion

5.1. Longitudinal samples

According to the mechanical behaviour and the microstructure presented in the previous section, we propose the following model:

The main relaxation mechanism of AISI 316 L is the movement of dislocations. The driving forces of this mechanism are the testing temperature, the applied stress, and the obstacles to be surmounted (precipitates inside the grains and at grain boundaries). When the energy barrier set by the obstacles is greater than the energy provided by the driving forces, we then say that the obstacles anchor the movement of the dislocations. The relaxation due to this mechanism can be well described by Johnston-Gilman's equation. At any given time all the intragranular precipitates—either in longitudinal or transverse samples—delay or impede the dislocation movements, disregarding which thermal treatment was previously applied. At low applied stresses there are not enough mobile dislocations for us to appreciate a measurable relaxation, as shown for samples type AR 137 MPa in Fig. 1(a). However, when the applied stress and consequently the number of unpinned dislocations increases, a certain stress relaxation is observed, as illustrated in Figs. 1(a) and (b).

The driving forces can act through another deformation mechanism [2, 3]: sliding at grain boundaries. Relaxation through this mechanism usually appears at high homologous temperatures and is well fitted by the high-homologous temperature branch of Hart's equation. It should be pointed out that, even when tests were not performed at high temperatures, grain boundary sliding is the only possible mechanism of deformation when the precipitates inside the grains anchor dislocations. This is clearly seen in the relaxation of samples subjected to the heat treatment at the lowest temperature and bent under intermediate stresses, Fig. 3(a), and at the beginning of the relaxation curves with double curvature

as illustrated in the relaxation of samples type *C* in Fig. 3(b). We therefore conclude that the changes in the internal stress are due to the precipitate-matrix interface. This fact is more comprehensible if we consider the minima free energy and contact angle of the second phase.

5.2. Transverse samples

By simple observation we could determine that the relaxation curves were concave upwards figures 4(a) and (b), and so the Johnston-Gilman model is the appropriate for fitting data in this particular case (this model has already been explained in a previous paragraph). Considering the characteristic m parameter of this model, relaxation curves may be arranged into two groups, each one of them characterized by a different m value.

The first group, with $m = 3$, has a microstructure consisting of very fine precipitates of titanium, (Cr,Mo) carbides and a sigma phase. Precipitates were found both inside the grains and at their boundaries, as shown in figure 8.

The second group, represented by the stress parameter $m = 2$, presents $M_{23}C_6$ and MC precipitates as well as sigma phase precipitates, as depicted in Fig. 9. The latter were extremely small (in the order of a micron) and were present at a much lower density than in the $m = 3$ samples. In all of the cases studied the interior of the grains represents the favourite nucleation site. Although a few precipitates were found at grain boundaries, these did not represent an obstacle for the movement of dislocations. Consequently, the deformation speed is greater than in the $m = 3$ case, because the dislocations can slide easily and their movement is not affected by the presence of the precipitates.

That the existance of an effective precipitatés size that does not interfere with the sliding of dislocations is clear; even when they coarse slowly, if they are to adopt a larger size, they can become walls for the dislocations to climb-this is in fact the case of the titanium and (Cr, Mo) carbides present in the $m = 3$ samples.

We can finally conclude that the m parameter seems to be in some way related to the amount of second phase precipitates found at grain boundaries. At the same time, this parameter shows no dependence on the tension applied by the holders- this last being the main parameter of the tests of our analysis.

6. Conclusions

Two phenomenological models, developed by Johnston-Gilman and Hart, are suitable to explain the stress relaxation in bending of AISI 316 L at 773 K. Our proposal puts forward that the Johnston-Gilmanés model is useful when the relaxation mechanism consists in the movement of dislocations controlled by precipitates inside the grains. On the other hand, Hart's model applies when the obstacles to overcome to observe relaxation of the microstructure are precipitates at grain boundaries.

Aknowledgments

Authors wish to thanks authorities of Instituto Argentino de Siderurgia, in which the researchers developed part of this investigation, through the agreement with Facultad Regional San Nicolás – Universidad Tecnológica Nacional

References

1. F. R. N. NABARRO, *Metallurgical and Materials Transactions* A **33A** (2002) 213.
2. I. M. LIFSHITZ, *Sov. Phys. JETP* **17** (1963) 909.
3. T. G. LANGDON, *Metallurgical and Materials Transactions* A **33A** (2002) 249.
4. E. I. SAMUEL, B. K. CHOUDHARY and K. BAHNU SANKARA RAO, *Scripta Materialia*, **46** (2002) 507.
5. K. G. SAMUEL, S. L. MANNAN, P. RODRIGUEZ and V. M. RADHAKRISHNAN, *Journal of Mater. Science* **30** (1995) 1521.
6. F. C. MONKMAN and N. J. GRANT, *Proc. ASTM* **56** (1986) 593.
7. W. G. JOHNSTON and J. J. GILMAN, *Journal of Applied Phys.* **30** (1959) 129.
8. E. W. HART, *Journal of Eng. Mater. Technol.* **98** (1976) 193.
9. F. POVOLO and R. J. TINIVELLA, *Journal of Mater. Sci.* **19** (1984) 1851.
10. D. E. FRASER, P. A. ROS-ROS and A. R. CAUSEY, *Journal of Nucl. Mater.* **46** (1973) 281.
11. F. POVOLO and E. H. TOSCANO, *Journal of Nucl. Mater.* **74** (1978) 76.
12. F. POVOLO and R. J. TINIVELLA, *Journal of Mater. Sci.* **19** (1984) 2353.
13. F. POVOLO and J. F. REGGIARDO, *Journal of Mater. Sci.* **23** (1988) 241.
14. G. F. VAN DER VOORT, "Atlas of time-temperature diagrams for iron and steels" (Edited by American Society for Metals International, United States of America, 1991) 640.
15. D. N. WASNIK, G. K. DEY, V. KAIN and I. SAMAJDAR, *Scripta Materialia* **49** (2003) 135.

Received 18 May 2004
and accepted 7 July 2005